

# Sub-pixel Edge Detection of LED Probes Based On Partial Area Effect

Chung-Yen Su<sup>1</sup>, Li-An Yu<sup>1</sup>, Nai-Kuei Chen<sup>1</sup>, Jheng-Jyun Wang<sup>1</sup>, Ying-Hao Liu<sup>1</sup>, Shuen-De Wu<sup>2</sup>

<sup>1</sup>Department of Electrical Engineering, <sup>2</sup>Department of Mechatronic Engineering

National Taiwan Normal University, Taiwan

scy@ntnu.edu.tw, 40075024H@ntnu.edu.tw, 40075022H@ntnu.edu.tw, 40075041H@ntnu.edu.tw, 60275002H@ntnu.edu.tw, sdwu@ntnu.edu.tw

**Abstract**—In recent years, the demands for LED are increasing. For testing the quality of LEDs, a lot of LED probes are necessary, so the high precision and efficient methods are paid more attention by industrial applications. This paper is focused on the measurement of the angle and the radius of a LED probe by computer vision. In previous paper, we proposed an effective method based on Canny edge detection and curve fitting method with iteration. In this paper we add a new sub-pixel edge detection method: partial area effect. We improve the preciseness of angle from error 2.3% to 1.43% and enhance the accuracy of radius more than 30%.<sup>1</sup>

**Keywords**—Edge detection, Sub-pixel edge detection, Probe, LED

## I. INTRODUCTION

Edges are always in high frequency and located in high contrast region. Edge detection is the crucial step for many computer vision applications. Utilizing the characteristics of edges can help us to extract the objects from images, so determining the edge location fast and accurately is the main point for a measuring system.

The precision and accuracy is the main target of measuring LED probes. In order to test a LED probe's angle and radius, as shown in Fig. 1, the input images from camera have to be processed, including filtering, edge detection, sub-pixel edge detection, and so on.

Detecting the edge of a LED probe generally has the following five main steps.

- Step 1: Use a low-pass filter to reduce the noise.
- Step 2: Detect coarse edge points by a pixel level edge detection.
- Step 3: Classify the coarse edge points to get three groups. Two groups of them are used to estimate the angle and one is used to estimate the radius, respectively.
- Step 4: Use a sub-pixel edge detection to improve the coarse edge points.
- Step 5: Use the curve fitting algorithm to determine the angle and the radius.

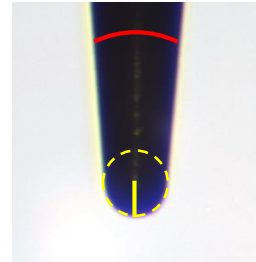


Fig. 1. The solid lines with red and yellow are angle and radius of a LED probe, respectively.

The commonly used filters to reduce noise are mean filters and Gaussian filters [1, 2]. Coarse edge detection can be performed by using the general operators including Sobel, Scharr, Laplacian of Gaussian (LOG), and Canny. These operators are efficient on edge detection, but the positions of detected edge points are all in pixel level.

To increase the precision of edge detection, several sub-pixel techniques had been proposed, including curve-fitting, moment-based [3-6], reconstructive [7] and partial area effect methods [8]. These methods have their characteristics. Curve-fitting methods are computationally simple but are easily affected by noise. Moment-based methods use integral pixels to reduce the effect of noise but require more computations. Reconstructive methods use horizontal gradients or vertical gradients to build a curve and find the peak of the curve as the sub-pixel edge. Partial area effect methods require different sizes of blocks to serve as horizontal and vertical models.

In literature, Tabatabaie and Mitchell were first two people to use sub-pixel technique to increase precision of edge detection. In [3], a Zernike orthogonal moment-based (ZOM) method is proposed for sub-pixel edge detection. The property of ZOM is rotation invariant and it is useful for pattern recognition and matching. In [4], Bin *et al.* proposed a method of detecting sub-pixel edges based on Fourier-Mellin Moment (OFMM). This method has a great ability to describe tiny things. In order to reduce the computational complexity, some researchers used Sobel operator to determine coarse edges before using moment-based sub-pixel methods [5, 6]. Recently, Trujillo-Pino *et al.* [8] proposed a new sub-pixel detection method based on partial area effect and showed that it is effective for camera captured images with apparent boundary.

Motivated by the partial area effect method, we add it to our previous method [9] and then compare its results with other

<sup>1</sup> This work is partly supported by National Science Council under Contract No. NSC 102-2218-E-003-001-MY2

sub-pixel methods. Finally, we conclude the better method for measuring the LED probes.

This paper is organized as follows. Section 2 consists of the basic information about sub-pixel edge detection. Section 3 details the proposed method. Section 4 shows the experimental results with three different methods. We make the concluding remarks in the last section.

## II. SUB-PIXEL EDGE DETECTION

Although edge-detection methods can get the coarse edges of an object, the level of the edge information is in pixel. In order to enhance the precision of edge points, we use sub-pixel techniques, including iterative curve-fitting and partial area effect methods. We briefly introduce these sub-pixel edge detections as follows.

### A. Iterative curve-fitting

For a curve-fitting method, we build a model by using edge points (see Fig. 2). Let the sum of squared errors between the edge points and the model be the smallest. Then the model is the best fit to these edge points. It is easy to compute the parameters of the model.

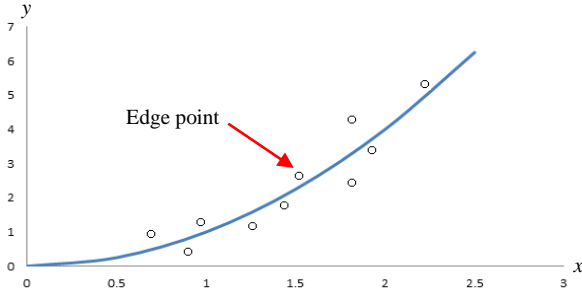


Fig. 2. Blue line shows the best fit of the edge points.

In order to reduce the effects of badly defined edge points on straight line, we calculate the standard deviation with the equation of line  $L_1$  which is calculated by curve-fitting method at first. Then we eliminate the points which are far from  $L_1$  (larger than two times of standard deviation). After that, the model of the best fit is recalculated. This process continues until the maximum number of iteration is reached or no more points are eliminated. We called the process as iterative curve-fitting method. With the iterative curve-fitting method, we can get a more accurate straight line than the first one we got.

### B. Partial area effect

We briefly introduce the method based on partial area effect herein. More details can refer to [8]. At first, we create the  $3 \times 9$  mask for the selected edge point and calculate  $dx$  and  $dy$  by Sobel operator to get the value of  $m$ , as shown in the following expressions.

$$m = 1 \quad \text{if } dx \times dy > 0 \quad (1)$$

$$m = -1 \quad \text{if } dx \times dy < 0 \quad (2)$$

Next, two constraints (see (3) and (4)) are used to check if one point's gradient is the local maximum or not. If the answer is yes, the direction of mask type is determined by comparing the values of  $|dx|$  and  $|dy|$ .

Constraint 1:

$$|dx(x-1, y)| \leq |dx| \text{ AND } |dx| \geq |dx(x+1, y)| \quad (3)$$

Constraint 2:

$$|dy(x, y-1)| \leq |dy| \text{ AND } |dy| \geq |dy(x, y+1)| \quad (4)$$

Mask type	Linear equation	Condition
Vertical:	$y = a + bx + cx^2$	$ dy  >  dx $
Horizontal:	$x = a + by + cy^2$	$ dx  >  dy $

If the mask type is vertical ( $|dy| > |dx|$ ), the  $y$  of  $x$  equation is used. Otherwise, the  $x$  of  $y$  equation is used instead. Each equation is assumed as a linear equation, as shown as above. The parameters ( $a$ ,  $b$  and  $c$ ) of each linear equation can be calculated from  $A$ ,  $B$ ,  $S_L$ ,  $S_M$  and  $S_R$  (see (5)-(7)).  $A$  and  $B$  are the average intensities of blue and green ranges in Fig. 3, respectively.  $S_L$ ,  $S_M$ , and  $S_R$  are the sum of intensities of the row in Fig. 3(a) or column in Fig. 3(b).

$$c = \frac{S_L + S_R - 2S_M}{2(A-B)} \quad (5)$$

$$b = m + \frac{S_R - S_L}{2(A-B)} \quad (6)$$

$$a = \frac{2S_M - 7(A+B)}{2(A-B)} - \frac{7}{12}c \quad (7)$$

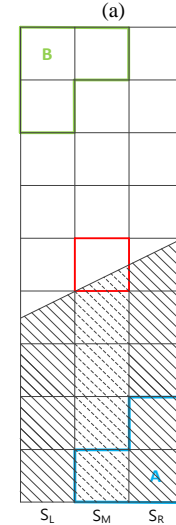
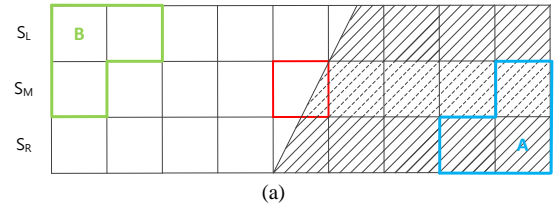


Fig. 3. Red block is the edge point. (a) and (b) are the different mask type of partial area effect method.

Finally, we can get the sub-pixel position of the edge point according to different mask type, as shown as below.

Mask type	Sub-pixel position
Vertical:	$(x, y + a)$
Horizontal:	$(x + a, y)$

### III. PROPOSED METHOD

At first, we briefly introduce our previous method [9]. Then, we depict the differences between the previous method and the proposed method.

In [9], we reduced the noise by using a mean filter to the gray-level images captured from the camera. Next, we used Canny edge detection to get coarse edges and Sobel operator to compute gradient directions. The directions are used to classify the edge points into three groups, namely left line group, right line group, and circle group. Finally, we used the aforementioned iterative curve-fitting method to calculate the angle and the radius of a LED probe.

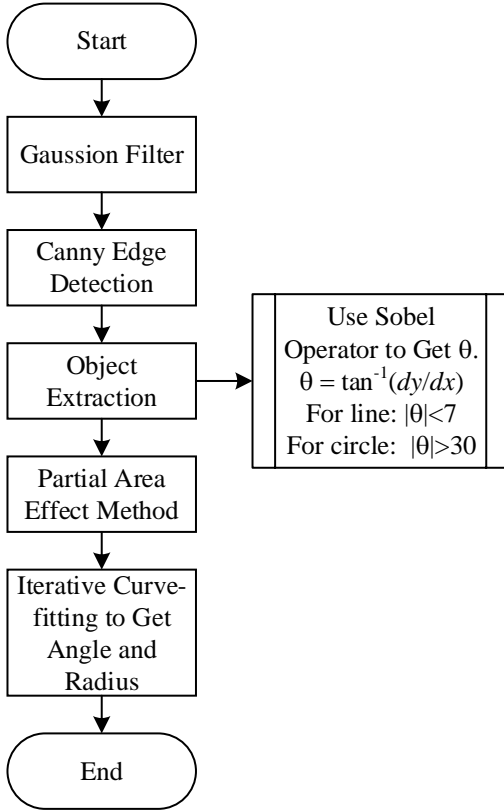


Fig. 4. Flow chart of the proposed method.

Figure 4 shows the flow chart of the proposed method. We replace the mean filter by a  $5 \times 5$  Gaussian filter. We still use Canny edge detection to find the coarse edge points but set its high and low thresholds automatically to increase the efficiency during processing. We calculate the mean intensity of a gray image and multiply the mean intensity by 0.3 to serve

as the high threshold and by 0.1 to serve as the low threshold, respectively.

The coarse edge points will be classified into three groups. First, we use the middle position of the probe to separate the points into right points and left points. Next, we get the gradient direction  $\theta$  of each point from Sobel operator by using

$$\theta = \tan^{-1} \frac{dy}{dx} \quad (8)$$

where

$$dx = f(i, j) * \begin{bmatrix} -1 & 0 & 1 \\ -2 & 0 & 2 \\ -1 & 0 & 1 \end{bmatrix}$$

and

$$dy = f(i, j) * \begin{bmatrix} -1 & -2 & -1 \\ 0 & 0 & 0 \\ 1 & 2 & 1 \end{bmatrix}.$$

Herein,  $f(i, j)$  denotes the image pixel value and the notation “\*” denotes the convolution.

Compared with the previous method [9], the proposed method modifies the conditions in the object extraction. The new conditions are as follows. If the absolute value of a point's direction is smaller than 7 degree,  $|\theta| < 7^\circ$ , the point is classified into the line groups. On the other hand, if the absolute value of a point's direction is above 30 degree,  $|\theta| > 30^\circ$ , the point is classified into the circle group (the front of a probe). A point that does not fit these two conditions is discarded. Note that these conditions are made by the experiment. We found that a vertically placed probe has an angle, which is always smaller than  $14^\circ$ , as shown in Fig. 5. By using the proposed conditions, we can get the three groups of edge points for a real probe, as illustrated in Fig. 6.

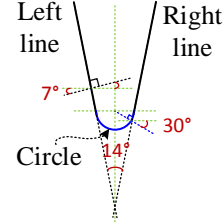


Fig. 5. The gradient directions of lines and the front of the probe.

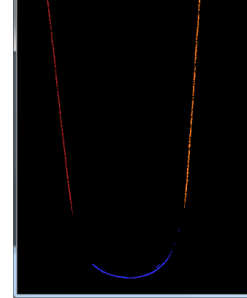


Fig. 6. Left line, right line and circle groups are illustrated in red, orange and blue colors, respectively.

After getting the edge points, we use the partial area effect method in [8] to the original grey-level image and focus on finding the sub-pixel edges of the image. However, we remove the two constraints (Eqs.(3) and (4)) in the proposed method. For a camera captured image, we found that the edge is blurry

and occupies a wide range, as shown in Fig. 7. With the two constraints, many non-local maximum edge points will be eliminated. For example, there are twelve edge points found from the Canny edge detection as shown in Fig. 8 and seven of them are eliminated from the constraint in (3).

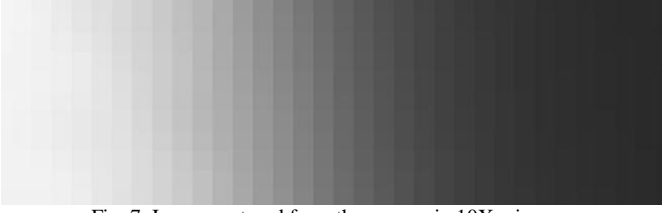


Fig. 7. Image captured from the camera in 10X microscope.

10	16	35	54	66	75	77	81	88	89	96	103	101	96	84	73	71	66	55	45	41	31
17	21	32	51	67	72	72	79	85	88	99	106	103	95	81	75	75	66	54	44	39	32
26	26	27	46	66	69	68	76	83	88	101	110	104	93	80	76	76	67	55	45	38	32
30	26	23	45	67	68	64	72	83	89	102	112	104	92	81	76	76	69	56	47	40	32
28	22	24	47	68	68	61	70	86	90	100	111	105	93	83	77	76	70	57	49	42	32
24	22	29	47	65	68	62	71	87	89	97	108	106	95	85	81	77	69	59	51	41	32
21	27	35	44	57	67	68	74	84	88	95	103	105	97	88	86	79	69	61	51	39	32
19	31	40	41	49	65	73	77	83	89	92	98	104	98	90	88	81	71	63	50	37	32
17	32	42	40	46	63	71	76	87	92	90	96	103	97	89	88	82	71	64	52	37	32
16	32	41	40	46	60	66	73	90	95	92	97	102	96	88	87	80	69	64	55	40	33
17	31	39	40	45	56	64	73	89	95	94	99	103	96	89	86	77	68	64	56	42	35
18	29	37	40	44	53	64	75	88	93	92	99	104	96	90	87	78	69	63	55	42	37
15	28	37	41	44	51	63	75	88	92	89	98	105	96	87	86	82	72	63	54	42	38

Fig. 8. The shown value is  $|dx|$  of the Gaussian filtered image. The blue blocks are the edge points obtained by Canny edge detection and the blocks with a red circle will be eliminated with the two constraints.

Finally, we use the iterative curve-fitting method to get two linear equations (see (9) and (10)). One is calculated from the points in the left line group, and the other is calculated from the points in the right line group.

$$\text{Left line: } y = m_1x + e \quad (9)$$

$$\text{Right line: } y = m_2x + f \quad (10)$$

where  $m_1$  and  $m_2$  are the slopes of the lines, and  $e$  and  $f$  denote the corresponding intercepts.

After getting these parameters of lines, we can get the angle of the probe by using the cosine theorem.

$$\theta = \cos^{-1}\left(\left|\frac{m_1 \times m_2 + 1}{\sqrt{m_1^2 + 1} \times \sqrt{m_2^2 + 1}}\right|\right) \quad (11)$$

As for the radius, we build a circle model from the points in the circle group. The circle model is shown in (12). With it, we can get the radius of the probe from (13).

$$\text{Circle model: } x^2 + y^2 + dx + ey + f = 0 \quad (12)$$

$$\text{Radius: } R = \frac{1}{2} \sqrt{d^2 + e^2 - 4f} \quad (13)$$

## IV. EXPERIMENTAL RESULTS

In the experiment, we have 23 test images that are captured by a CMOS sensor camera. The size of the images is 1920×1080. Some of the images are shown in Fig. 9. Since these images are captured in BGR format, we need to transform them to get their corresponding grey-level images first. Then we use the proposed method to calculate the angle and the radius of each LED probe. We set the maximum number of iteration in the iterative curve-fitting method to five. Table I tabulates the experimental results. In the table, we also list the results of [8] and [9] for comparison. The referred values are measured from a SEM (Scanning Electron Microscope) system. For the step of sub-pixel edge detection, the proposed method is different from [8] in the two constraints. We do not use these two conditions to avoid removing too much points, leading to a worse result. For clarity, we mark the best values of angle error and radius error for each sample image in red digits.

As we can see in the table, the proposed method generates most of the best results. The average angle errors are 2.3% for [9], 1.54% for [8], and 1.43% for the proposed method, respectively. Thus, the proposed method has the smallest average angle error. As for the average radius errors, they are 37.22% for [9], 1.61% for [8], and 1.43% for the proposed method, respectively. Likely, the proposed method has the smallest average radius error. Note that the method in [9] has a quite large radius error because it uses a different scheme to determine the thresholds of Canny edge detection and it does not use any sub-pixel edge detection to refine the locations of edge points.

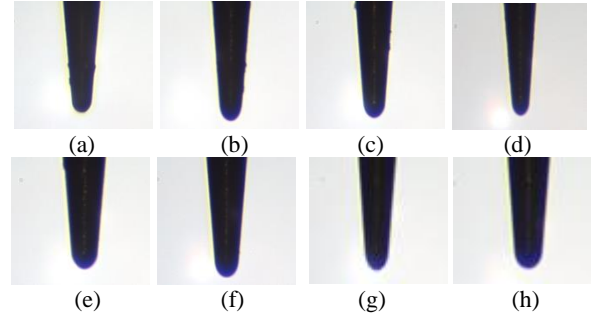


Fig. 9. (a), (b), (c), (d), (e), (f), (g) and (h) are samples from 1 to 8, respectively

## V. CONCLUSION

In this study, we proposed a method to determine the edge locations with sub-pixel accuracy for the application of LED probes. In the proposed method, we use Canny edge detection to find coarse edge points after using a Gaussian filter to reduce the noise. Next, we classify the points into three groups and discard remaining points. We refine the edge location of each point by using the partial area effect method without two constraints. Finally, we calculate the angle and the radius of a probe by using the iterative curve-fitting. Experimental results show the effectiveness of the proposed method.

Table 1 Experimental results of different sub-pixel edge detection methods

Items Image	Referred values		[9]		[8]		Proposed method	
	Angle (degree)	R (um)	Angle Error (%)	Radius Error (%)	Angle Error (%)	Radius Error (%)	Angle Error (%)	Radius Error (%)
sample1	10.1	16.75	1.98	14.09	1.97	0.55	1.91	0.01
sample2	10.3	20.75	1.65	100	1.1	2.1	0.96	2.17
sample3	10.2	21.25	2.06	0.85	2.43	0.9	1.91	3.06
sample4	10.3	15.25	1.94	8.72	1.76	0.47	1.36	0.79
sample5	10.7	23.25	0.75	12.47	0.44	4.49	0.11	1.91
sample6	9.6	25.25	1.98	3.25	0.57	0.16	0.6	0.27
sample7	10.5	22.25	0.76	41.44	1.13	1.78	1.09	1.91
sample8	10.4	22.75	0.87	20.22	0.52	2.43	0.42	2
sample9	10.1	23.25	2.87	11.78	1.83	2.56	1.77	3.68
sample10	10.1	22.25	2.57	91.51	1.79	0.54	1.64	0.01
sample11	9.4	22.75	3.83	1.23	3.61	0.89	3.39	0.06
sample12	10.2	24.75	1.18	76.32	0.36	0.81	0.16	0.26
sample13	10.1	23.75	1.98	24.59	1.86	1.54	1.52	0.02
sample14	10	21.25	2.3	13.13	1.8	0.16	2.1	1.1
sample15	10.1	23.75	1.78	100	1.45	2.35	1.61	2.21
sample16	10.7	23.75	3.18	56.63	2.27	6.83	2.28	7.04
sample17	10.3	22.75	0.29	19.6	0.17	0.41	0.3	0.75
sample18	10.2	23.25	3.14	87.53	3.17	0.66	3.01	0.67
sample19	9.7	23.75	10.72	100	0.34	1.15	0.21	1.15
sample20	10.2	23.25	2.75	22.75	2.4	2.64	2.15	1.99
sample21	9.7	22.25	0.62	10.65	0.61	1.62	0.81	0.79
sample22	10.3	22.25	2.23	7.55	1.9	0.73	1.69	0.61
sample23	9.8	23.75	1.53	31.83	2	1.33	1.91	0.47
Average			2.3	37.22	1.54	1.61	1.43	1.43

## REFERENCES

- [1] R. C. Gonzalez and R. E. Woods, "Digital Image Processing," 3<sup>rd</sup> Edition, *Prentice-Hall, Inc.*, 2008.
- [2] R. C. Gonzalez, R. E. Woods, and S. L. Eddins, "Digital Image Processing-using MATLAB," Edition, *Prentice-Hall, Inc.*, 2004.
- [3] S. Ghosal, R. Mehrotra, "Orthogonal moment operators for subpixel edge detection," *Pattern Recognition*, 26 (2), pp.295-306, 1993.
- [4] T. J. Bin, A. Lei, J. W. Cui, W. J. Kang, D.D. Liu, "Subpixel edge location based on orthogonal Fourier-Mellin moments," *Image and Vision Computing*, 26 (4), pp. 563-569, 2008.
- [5] Y. D. Qu, C. S. Cui, S. B. Chen, J. Q. Li, "A fast subpixel edge detection method using Sobel-Zernike moments operator," *Image and Vision Computing*, 23 (1), pp. 11-17, 2005.
- [6] Z. F. Hu, H. S. Dang, X. R. Li, "A novel fast subpixel edge detection method based on Sobel-OFMM, " in *Proc. of IEEE International Conference on Automation and Logistics*, pp. 828-832, 2008.
- [7] A. Fabijańska, "A survey of subpixel edge detection methods for images of heat-emitting metal specimens," *International Journal of Applied Mathematics and Computer Science*, vol. 22, no. 3, pp. 695-710, 2012.
- [8] A. Trujillo-Pino, K. Krissian, M. Alemán-Flores, D. Santana-Cedrés, "Accurate subpixel edge location based on partial area effect", *Image and Vision Computing*, 31, pp. 72-90, 2013.
- [9] N. Q. Chen, J. J. Wang, L. A. Yu, and C. Y. Su, "Sub-pixel Edge Detection of LED Probes Based on Canny Edge Detection and Iterative Curve Fitting", in *Proc. of IEEE International Symposium on Computer, Consumer and Control*, pp. 131-134, 2014.